Acta Polytechnica **65**(1):1–8, 2025
https://doi.org/10.14311/AP.2025.65.0001

Published by the Czech Technical University in Prague

THE SPATIAL DISTRIBUTION OF GRBS

Zsolt Bagoly[a,b,*], Lajos G. Balazs[d,e], Zsuzsa Horvath[c], Istvan Horvath[a]

[a] *University of Public Service, Department of Natural Sciences, 2 Ludovika tér, H-1083 Budapest, Hungary*

[b] *Eötvös University, Faculty of Science, Department of Physics of Complex Systems, Pázmány Péter sétány 1/A, H-1117 Budapest, Hungary*

[c] *University of Public Service, Institute of Disaster Management, 2 Ludovika tér, H-1083 Budapest, Hungary*

[d] *Eötvös University, Department of Astronomy, Pázmány Péter sétány 1/A, H-1117 Budapest, Hungary*

[e] *HUN-REN Research Centre for Astronomy and Earth Sciences, Konkoly Thege Miklós Astronomical Institute, Konkoly-Thege Miklós út 15-17, H-1121 Budapest, Hungary*

[*] corresponding author: bagoly.zsolt@uni-nke.hu

Abstract. We analysed the different aspects of the spatial distribution of 542 Gamma-Ray Bursts with precisely determined positions and spectroscopic redshifts. The data were divided according to the origin of the redshift (afterglow or host galaxy). The yearly rate of afterglow and host-based redshift observations are different, with only a few host observations in the recent years. Since the launch of the Swift, the rate of afterglow observations fall exponentially by 50 % in 15 years, potentially affecting all planned GRB missions. We also analysed the rest-frame T_{90} values from the Swift BAT and FERMI GBM catalogues with the redshift data. The host- and afterglow-based points are separated in the redshift range due to observational effects, but no direct distinction could be made between the rest-frame T_{90} values. The correlation analysis between the GRB redshift and sky position shows that the GRB distribution could be factorised into a separate sky and radial components.

Keywords: Data analysis, gamma-ray bursts.

1. Introduction

Gamma-ray bursts (GRBs) are ideal candidates for probing large-scale structures due to their ability to detect up to very high redshifts. According to the Cosmological Principle, the Universe is spatially homogeneous and isotropic on a large scale, and we believe that GRBs follow the distribution of baryonic matter. This allows us to use GRBs to test the baryonic matter's distribution in the Universe, especially the large-scale structure.

GRBs are assumed as one of the most powerful and extremely bright events in the universe, which are caused by a burst of massive stars [1, 2] or the merging of binary compact objects [3]. Therefore, the link between star formation events and long duration GRBs is thought to be strong, as they are thought to originate from hypernovae originated from regions of active star formation. Observations show that GRBs are more common in the early star-forming regions of galaxies (e.g. [4–6]), in low-metallicity environments. This low metallicity affects stellar winds, allowing massive stars to retain more mass until they explode. Since GRBs can be observed at great distances, they also act as probes for investigating star formation in the early universe.

The primary GRB groupings, notably the short and the long one, display diverse sky distribution, according to the early CGRO BATSE observations anisotropy investigations [7–13].

A huge GRB cluster at $z \approx 2$, located in the direction of Hercules and Corona Borealis, has been identified in [14], where 283 GRBs with redshifts were used to study their distribution. The GRB sample was split by z based on the assumption that sky exposure is independent from the radial distribution. The k-th closest neighbour analysis and the bootstrap point radius technique was used on the dataset. Nearest-neighbor studies confirm the previously discovered massive, loose GRB cluster in the redshift range $1.6 < z \leq 2.1$, with a $p = 1.6 \times 10^{-4}$ chance [15]. The original discovery was later supported by further data and analysis as new GRBs' redshift were observed [15, 16]. The exact nature of the structure remains unclear.

[17] further investigated the k-th nearest neighbor in the GRB sample, inspired by the Hercules-Corona Borealis Great Wall. Here, the GRBs' spatial density was approximated using the k-th Next Neighbour Statistics, rather than redshift space slices. They discovered that for $k = 8, 10, 12$, and 14, the analysis revealed the Giant GRB Ring, consisting of 9 GRBs with an angular major/minor diameter of 43°/30° at a distance of $\approx 2\,770$ Mpc in the $0.78 < z < 0.86$ redshift range, with a probability of 2×10^{-6} of being a random fluctuation. [18] analysed the spatial point processes of GRBs with known redshifts with kernel smoothing. They concluded that the occurrence of the Giant GRB Ring is a low-probability random

event, as only three ring-like patterns were revealed from 1 502 random datasets. [19] investigated the distribution of starburst galaxies from the Millennium XXL simulation at $z = 0.82$ distance, but the actual origin of the Giant GRB Ring is still unclear.

[20] analysed the FERMI GBM data for sky distribution isotropy. The two-point angular correlation function was unable to identify statistical anisotropy for the both long and short GRBs due to a significant positional uncertainty. In [21], 6 289 GRBs were studied for their intrinsic features, including prompt and afterglow metrics, to determine relationships with GRB categorisation. [22] and [23] used Platinum GRB data compilation to standardise events in the Dainotti correlation space, resulting in GRB cosmological parameter limits consistent with BAO data. Also, the Fermi GBM GRB catalogue was used by [24] to evaluate the correlation between the sky locations of GRBs and their durations, fluences, and peak fluxes. [25] added the BATSE and Swift BAT GRBs to the data. The results of the studies reveal no connection between the GRBs' physical characteristics and their places in space.

The GRB clustering might have several astrophysical causes. Because of the extended inspiraling duration of the pair, short GRBs are not predicted to trace star-forming activity, but the low metallicity massive stars are thought to represent a long GRB progenitor. [26] analysed a Swift GRB sub-sample composed by 58 bursts with redshifts, favourable observing conditions, and 1-s peak fluxes above $2.6\,\mathrm{pg\,s^{-1}\,cm^{-2}}$. They found that strong evolution either in luminosity or in density is required to describe the sample. [27] using the same sample found that the GRB formation rate increases with up to $z \approx 2$, then drops with the star formation rate. However, [28] asserts, based on the findings of the Swift GRB Host Galaxy Legacy Survey, that long GRBs are not directly a trace of star formation as metallicity is the key factor the production efficiency. Using the Millennium Simulation [29], [17] showed that galaxies with a typical star creation rate compared to those with a high star formation rate likely have distinct spatial distributions. Therefore, theories regarding a wave or variation in the rate of star creation are too simplistic to fully capture the picture.

A possible origin might be genuine cosmic anisotropy. For instance, [30] examined anisotropic cosmic expansions using electrodynamics and forecasted changes in the polarisation of electromagnetic radiation in relation to these areas. In order to establish scaling relations, [31] examined 570 clusters using at least X-ray, microwave, and infrared observations. They found an apparent 9 % dipole-like spatial fluctuation in the local H_0 at $(l, b) = (280, 15)$ on the sky using all of the distance data that was available. Another explanation for the outcome might be a bulk flow of $900\,\mathrm{km\,s^{-1}}$.

2. Data selection

This paper uses different redshift observation of GRBs, most of which were triggered by NASA's Swift and/or Fermi satellites. All of them has precise spectroscopic redshifts originated from either optical afterglows or host galaxy measurements, with the corresponding investigations and locations on the celestial sphere.

We used the spectroscopical redshifts of 542 GRBs up to 31$^{\mathrm{st}}$ August 2022 from [16]. It has been extended with the data of [32] and [33] and the Gamma-Ray Burst Online Index (GRBOX) database. GRBOX also relies on the relevant Gamma Ray Burst Coordination Network (GCN) reports – here the GCN data were also used directly. A publicly available dataset compiled by Joachim Greiner, which provides extensive information on nearly all GRBs observed by any instrument was also used in addition to the GRBOX and were also cross-checked with our data.

Here, we used only the observations with spectroscopic redshifts, as photometric redshifts and redshift estimates (e.g. based on Ly-alpha limits) have large redshift (radial distance) uncertainties, exceeding several hundred Mpcs.

Figure 1, the galactic distribution of these 542 GRBs is shown. The colours are corresponding to the origin of the redshift (afterglow or host galaxy spectroscopy). There are 262/280 GRBs in the northern/southern Galactic hemisphere, and it is worth to mention that there are no visible difference between host- or afterglow-based positions.

3. Difference between host- and afterglow-based z

3.1. Redshift observations and their future

Using the collected data, one can determine the yearly variances of the redshift observations. The successful spectroscopic observations will be provided either by the rapid afterglow measurements (made within the afterglow dimming timeframe) or the host galaxy's spectral lines. The host galaxy could be observed later, and usually this is the case.

Figure 2, the yearly observation rates for the afterglow- and host-based redshifts and for all spectroscopic redshift are shown. The launch of the Swift satellite is clearly visible in the 2005's rate.

One can also observe that the rates of the afterglow- and host-based redshift observations are different: the peak in the host-based observations are dropping, only a few GRBs were observed in the last years. Without dedicated observations there's a low chance to reverse this trend: these measurements require the largest telescopes, where the observing time is limited. Altough determined observers for ground optical follow-ups are still cruical, the new trigger sources of SVOM and Einstein Probe (beside Swift and Fermi) will hopefully expand the trigger alerts'

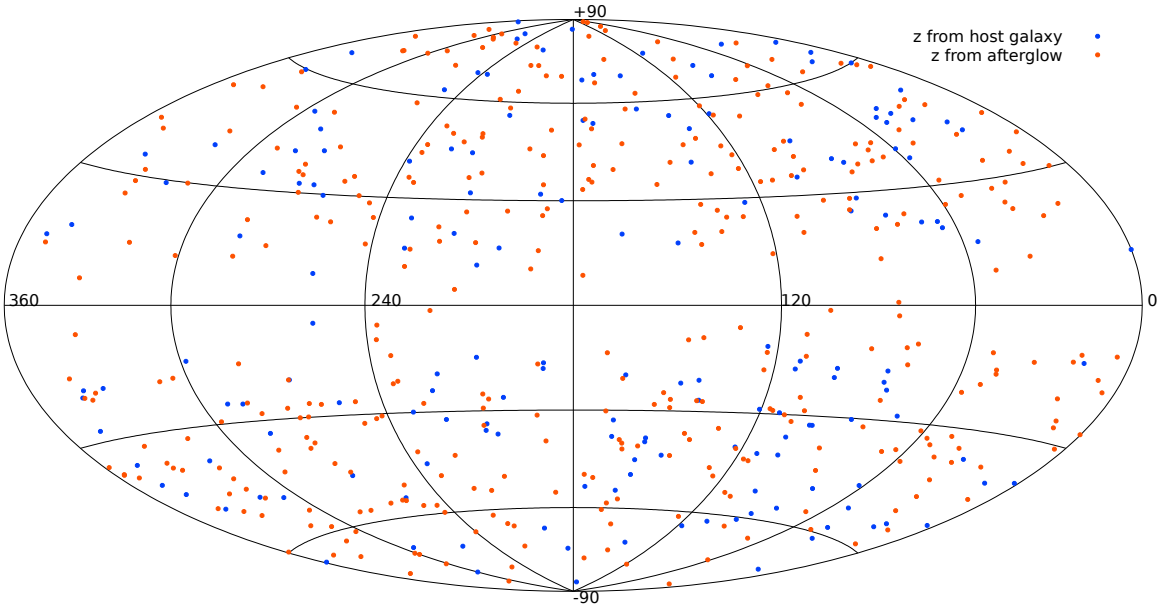

FIGURE 1. Sky distribution of 542 GRBs with measured redshift in galactic coordinates up to 31st August 2022. The disk of the Galaxy is clearly visible, it partially prevents the optical follow-up activity.

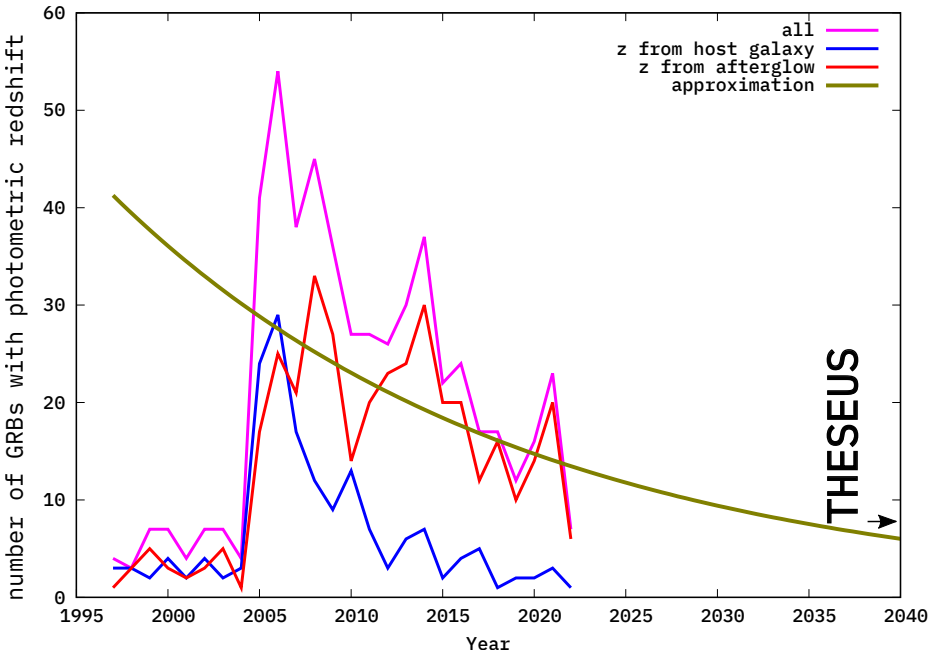

FIGURE 2. Yearly observation rates for the afterglow- and host-based redshifts and for all spectroscopic redshifts. Observation rate is clearly different for host- and/or afterglow-based redshifts. The exponential drop with a ≈15-year halving time means that during the THESEUS mission, only ≈5 redshifts are expected yearly.

rate, and planned missions like Theseus will further extend it in the next 10–15 years.

The drop in the number of the afterglow redshifts are clearly visible too: in ≈15 years, the number of observations decreased by ≈50 %. This lost interest in the GRB redshift determination could lead to a problem for all planned GRB missions, e.g. for Theseus the current estimation is ≈5 redshifts per year, clearly a critical situation endangering the mission's scientific output. This exponential decline in observer interest could be partially offset by rapid response/communication mechanisms: e.g. the fact that the succesful Swift XRT and UVOT afterglow detection will increase the chance of a spectroscopic redshift shows that for the success of Theseus, an on-board instrument such as IRT is central.

3.2. SELECTION EFFECTS IN THE REST-FRAME $T_{90} - z$ DISTRIBUTION

The short GRBs have a T_{90} duration of less than 2 seconds and have harder spectra compared to long GRBs. They are typically found in regions with low star formation rates, including older stellar populations and elliptical galaxies, which also support the view that

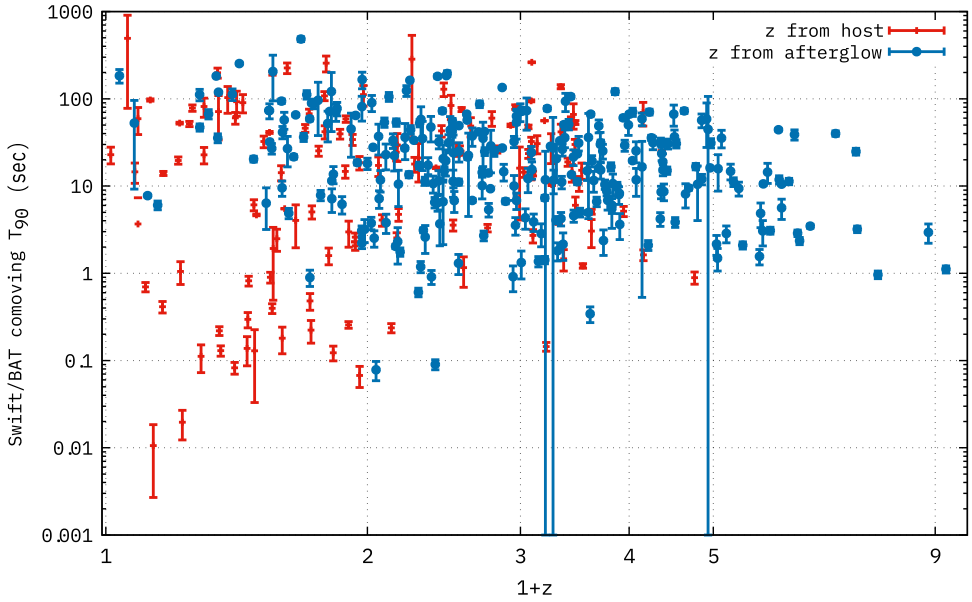

Figure 3. Swift BAT data's rest-frame T_{90} – z distribution of the dataset with the corresponding T_{90} errors (the errors in z are too small for this plot).

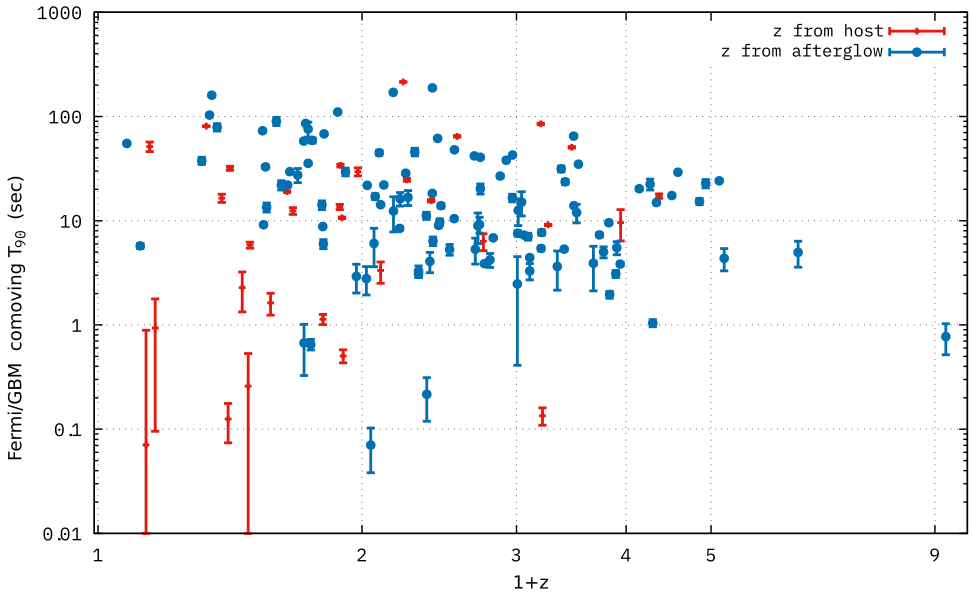

Figure 4. Fermi GBM data's rest-frame T_{90} – z distribution of the dataset with the correspondig T_{90} errors (the errors in z are too small for this plot).

they originate from the merger of compact objects, such as neutron stars or a neutron star and a black hole, The intermediate GRBs have a T_{90} duration between 2 and 10 seconds, with a soft spectra. The progenitors could be potentially a mix of mechanisms from both short and long GRBs or entirely different processes.

The long GRBs have a T_{90} duration of more than 10 seconds. They have been proposed to be associated with star-forming regions and the collapse of massive stars. The observed locations in galaxies with high rates of star formation, particularly in the arms of spiral galaxies also support this theory.

Using the redshift data and the published T_{90} durations from the Swift BAT and FERMI GBM catalogues one can plot the rest-frame T_{90} values with the redshifts (Figures 3–4). This method is clearly only the first approximation, considering the various observational effects, e.g. the varying detector background and/or the absence of proper K-correction of a light curve with various fast spectral changes.

The two satellites/detectors have different spectrum sensitivities and trigger conditions, therefore, the T_{90} values for the two figures cannot be directly compared (the relatively few shared observations were studied in detail by [34]).

GRBs' host galaxies have been barely seen above $z > 3$. The majority of short GRBs are observed by the Swift BAT and they clearly dominate the sub-second part of the plot.

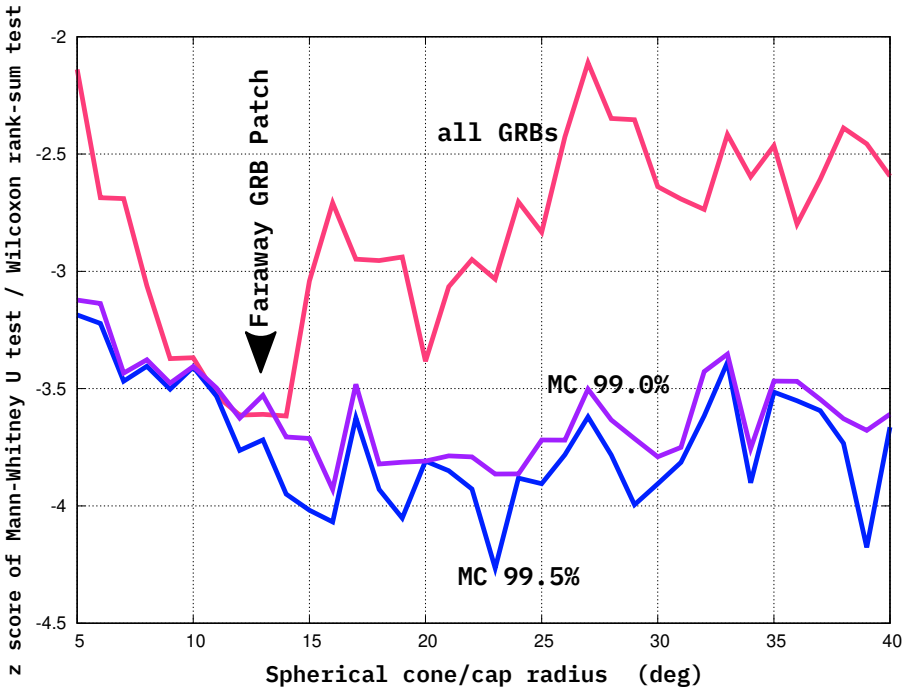

FIGURE 5. 542 GRBs' lowest Z scores and the MC 99 %/99.5 % estimate lines.

It is also apparent that while the restframe T_{90} values cover the same, wide, range, the host- and afterglow- based observations span across different redshift ranges. As a result, the various GRB types (short, intermediate, and long) ought to be contributed in both plots for the host and the afterglow observations.

The figures also show diverse trigger selection effects, such as missing medium/high-z short sources for both satellites. Full consideration of these observational factors is the topic of the ongoing research.

4. The factorisation of the GRB density function

Many factors, including geometrical factors, satellite activities, and optical follow-ups, affect the observational probability of a GRB on the sky, and it is an important question how the environment affects the observed GRB distribution.

To reconstruct the three-dimensional GRB distribution, it's important to determine if the sky distribution is independent of redshift/comoving radial distance. This involves evaluating the validity of the f (radial factor) $\times g$ (angular factor) expansion of the density function. We examined this association earlier in [33] by calculating the radial distance distribution of the nearby GRBs inside an α-sized spherical cap surrounding each GRB. Here, we repeat the test with the newly updated dataset.

The Mann-Whitney U test is a nonparametric test used to compare two samples (here the local data within a given spherical cap and the full radial distribution). It is not required that the data be normally distributed. The test joins the data from both groups and rank all the values. Using these ranks, it calculates the U statistic first:

$$U_1 = n_1 \cdot n_2 + \frac{n_1 \cdot (n_1+1)}{2} - R_1,$$
$$U_2 = n_1 \cdot n_2 + \frac{n_2 \cdot (n_2+1)}{2} - R_2,$$

where

n_1 is the number of observations in group 1,

n_2 is the number of observations in group 2,

R_1 is the sum of the ranks for group 1,

R_2 is the sum of the ranks for group 2.

The smaller value between U_1 and U_2 is used as the test statistic U.

The Mann-Whitney U-test's Z score is used to compare the data in the two samples:

$$\mu_U = \frac{n_1 \cdot n_2}{2},$$
$$\sigma_U = \sqrt{\frac{n_1 \cdot n_2 \cdot (n_1+n_2+1)}{12}},$$
$$Z = \frac{U-\mu_U}{\sigma_U}.$$

Probability was obtained with Monte Carlo mixing/randomisation between the radial (redshift) values and the positional data. The Z score distribution for a whole random local dataset were determined. The same procedure was repeated for 1 000 random datasets, each for $\alpha = (5-50)$ degrees radius. Figure 5 shows the results for our dataset, which include the least Z score from the real data (the second smallest values are above the 99 % curve of the Monte Carlo

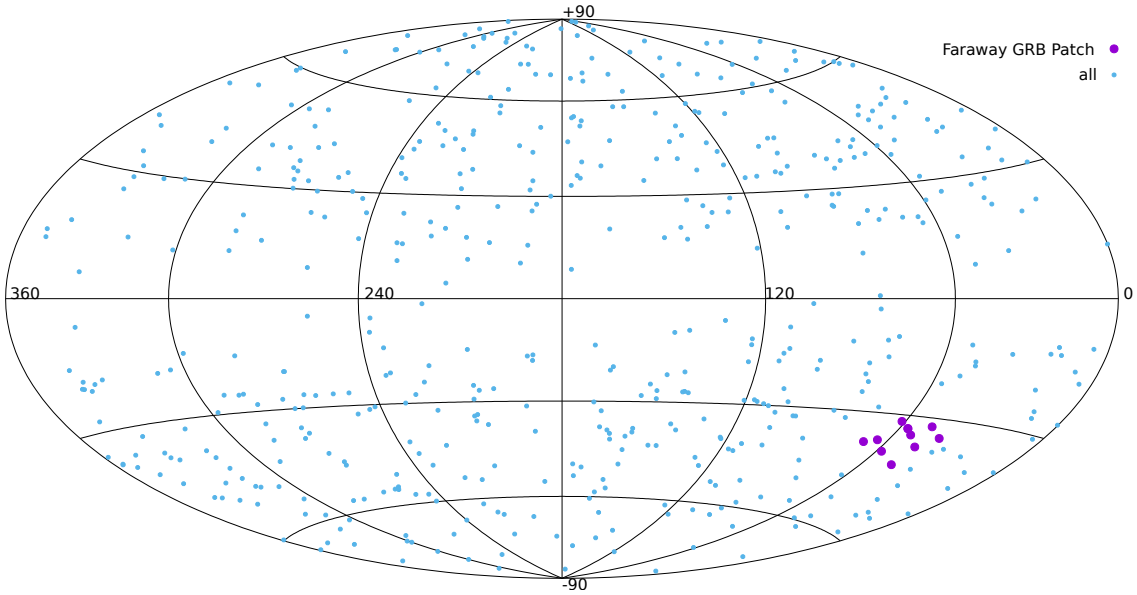

Figure 6. The sky distribution of the Faraway GRB Patch.

simulations). A spherical cap size of 12–14 degrees reveals an interesting location (the Faraway GRB Patch, Figure 6), with a matching random probability of 1 %.

Considering the significance of the result, it is important to recall that 542 separate tests were made, all of them centred on a GRB. Therefore, there is a strong correlation between the tests because of the overlapping data. There are ≈60 separate regions on the sky for the 12–14 degree size, therefore, there should be a correction factor with this minimum value. It is important to note that [33] only included 522 GRBs; in this case, the larger dataset resulted in a greater probability, which decreased the significance. Thus, according to this analysis, we may conclude that factorisation is not inconsistent with the observational data.

5. The bootstrap point-radius method

In [34], the point radius bootstrap method was applied to test for clustering in the redshift data. Using the results in [33], it assumed that the sky exposure is independent of z in order to use the point radius bootstrap approach. The preceding section's results support this factorisation, therefore, we describe the present status of the investigation.

The point radius bootstrap approach determines the distribution of GRBs inside a predetermined angular radius circle, which is parameterised by their A surface. Sliding the starting point k in redshift will select n consecutive GRB, in the radial distribution. All the GRBs inside the A cap will have the same sky exposure, therefore, the numbers of GRBs within and outside the redshift slice will allow us to check the uniformity of the radial distribution. We search for the greatest number of GRBs (K) for each radial beginning point k and for each GRB within the given A spherical cap. The spherical cap area of A and the slice size, n, are fixed parameters for a specific test.

A Healpix partition with 49 152 positions provides a quasi-isotropic distribution of the centre of the spherical caps, yielding an average centre distance of approximately 10 times lower than the average distance between the GRBs.

A Monte-Carlo simulation is performed, repeatedly mixing radial and angular locations a thousand times. The maximum number of GRBs detected within the angular circle is taken from these 1 000 examples and compared with the actual K values. It is important to note that the distribution should be comparable for similar k and A values.

The distribution of K is non-linearly dependent on the angular two-point correlation function both inside and outside the radial slice. However, the relationship between the spatial correlation function and the geometrical change in the angular diametre distance with the co-moving distance is quite complicated.

The [34] study uses a bootstrap approach to determine the likelihood of receiving a number K for a given n and A, analysing the GRBs in the galactic hemispheres separately.

For the northern galactic hemisphere clustering occurs on three angular separation range scales, indicating considerable departures from isotropy/homogeneity. The first of these range scales occurs for $n = 5$ and $A = 0.0628$. The analysis found one occurrence (0.0628, 5) where the bursts are located within a $0.59 \leq z \leq 0.62$ redshift range, with a likelihood of this fluctuation occurring by chance is of only 0.012.

The second of these angular separation ranges is around $41 \leq n \leq 47$, $1.6 \leq A \leq 1.9$. Only two neighbouring points achieve the least significant limit in a larger (n, A) region ($36 \leq n \leq 57$, $1.57 \leq A \leq 1.95$). $A = 1.7$, $p = 0.038$ for $n = 43$ and $p = 0.048$ for

$n = 43$ for $A = 1.728$. The redshift range of this cluster is $0.9 \leq z \leq 1.3$. These GRBs are located in the same sky location as the Hercules-Corona Borealis Great Wall, however, the latter is further away ($1.6 < z < 2.1$) [16]. The second section is included in the third since it covers the $z = 0.9$–2.1 range.

In the southern hemisphere, there are two possible clusters. One contains the Giant GRB Ring [17] around redshift of $z = 0.75$–0.86, with 9 out of 19 GRBs on only 0.4396 sr in the sky. The second has 24–29 GRBs with redshifts ranging from 0.55 to 1.17–1.25, with a corresponding probability above 3 %.

6. Conclusion

The yearly variances of redshift observations can be separated into two groups according to the afterglow measurements or the observation of the host galaxy's spectral lines. The rates of afterglow- and host-based redshift observations differ, with only a few host-based GRB redshift observed in recent years. The number of afterglow redshifts has decreased exponentially, by 50 % in 15 years, potentially affecting all future GRB missions. This decrease in observer interest can be partially compensated by rapid response/communication mechanisms, such as successful Swift XRT and UVOT afterglow detection, which raises the chance of a spectrosopic redshift.

We plotted the rest-frame T_{90} values using redshift data and published T_{90} durations from the Swift BAT and FERMI GBM catalogues as a first approximation for the analysis of the various observational effects. The host- and afterglow-based points are separated in the redshift range due to observational effects, but no direct disctintion could be made among the rest-frame T_{90} values. The study also shows diverse trigger selection effects, such as missing medium/high-z short sources for both satellites.

The observational likelihood of a GRB on the sky is influenced by various effects, such as satellite activity and optical follow-up factors (weather, telescope availability, observer activity, etc.). To reconstruct the three-dimensional GRB distribution, it is crucial to determine if the sky distribution is independent of redshift. The Mann-Whitney U test was used to compare the local redshift distribution within a given spherical cap and the full radial distribution. The probability was obtained with Monte Carlo mixing/randomisation between radial and positional values. The Z score distribution selected only one suspicious spherical cap area with radius of 12–14 degrees with a random probability of 1 %. Because the strong correlation between the tests due to the overlapping data results in a greater probability, decreasing the significance. Thus, factorisation is not inconsistent with the observed data.

Acknowledgements

The authors thank the Hungarian TKP2021-NVA-16 and TKP2021-NKTA-64 programs for their support.

References

[1] S. E. Woosley. Gamma-ray bursts from stellar mass accretion disks around black holes. *The Astrophysical Journal* **405**:273–277, 1993. https://doi.org/10.1086/172359

[2] S. E. Woosley, J. S. Bloom. The supernova gamma-ray burst connection. *Annual Review of Astronomy and Astrophysics* **44**:507–556, 2006. https://doi.org/10.1146/annurev.astro.43.072103.150558

[3] E. Berger. Short-duration gamma-ray bursts. *Annual Review of Astronomy and Astrophysics* **52**:43–105, 2014. https://doi.org/10.1146/annurev-astro-081913-035926

[4] H. Dénes, P. A. Jones, L. V. Tóth, et al. Exploring the pattern of the Galactic HI foreground of GRBs with the ATCA. *Monthly Notices of the Royal Astronomical Society* **489**(3):3778–3796, 2019. https://doi.org/10.1093/mnras/stz2314

[5] P. Héraudeau, S. Oliver, C. Del Burgo, et al. The European large area ISO survey VIII. 90-µm final analysis and source counts. *Monthly Notices of the Royal Astronomical Society* **354**(3):924–934, 2004. https://doi.org/10.1111/j.1365-2966.2004.08259.x

[6] L. V. Tóth, G. Marton, S. Zahorecz, et al. The AKARI far-infrared surveyor young stellar object catalog. *Publications of the Astronomical Society of Japan* **66**(1):17, 2014. https://doi.org/10.1093/pasj/pst017

[7] L. G. Balázs, A. Mészáros, I. Horváth. Anisotropy of the sky distribution of gamma-ray bursts. *Astronomy & Astrophysics* **339**:1–6, 1998. https://doi.org/10.48550/arXiv.astro-ph/9807006

[8] D. B. Cline, C. Matthey, S. Otwinowski. Study of very short gamma-ray bursts. *The Astrophysical Journal* **527**(2):827–834, 1999. https://doi.org/10.1086/308094

[9] M. Magliocchetti, G. Ghirlanda, A. Celotti. Evidence for anisotropy in the distribution of short-lived gamma-ray bursts. *Monthly Notices of the Royal Astronomical Society* **343**(1):255–258, 2003. https://doi.org/10.1046/j.1365-8711.2003.06657.x

[10] A. Mészáros, Z. Bagoly, I. Horváth, et al. A remarkable angular distribution of the intermediate subclass of gamma-ray bursts. *The Astrophysical Journal* **539**(1):98–101, 2000. https://doi.org/10.1086/309193

[11] A. Mészáros, Z. Bagoly, R. Vavrek. On the existence of the intrinsic anisotropies in the angular distributions of gamma-ray bursts. *Astronomy & Astrophysics* **354**:1–6, 1999. https://doi.org/10.48550/arXiv.astro-ph/9912037

[12] V. F. Litvin, S. A. Matveev, S. V. Mamedov, V. V. Orlov. Anisotropy in the sky distribution of short gamma-ray bursts. *Astronomy Letters* **27**(7):416–420, 2001. https://doi.org/10.1134/1.1381609

[13] R. Vavrek, L. G. Balázs, A. Mészáros, et al. Testing the randomness in the sky-distribution of gamma-ray bursts. *Monthly Notices of the Royal Astronomical Society* **391**(4):1741–1748, 2008. https://doi.org/10.1111/j.1365-2966.2008.13635.x

[14] I. Horváth, J. Hakkila, Z. Bagoly. Possible structure in the GRB sky distribution at redshift two. *Astronomy and Astrophysics* **561**:L12, 2014. https://doi.org/10.1051/0004-6361/201323020

[15] I. Horváth, Z. Bagoly, J. Hakkila, L. V. Tóth. New data support the existence of the Hercules-Corona Borealis Great Wall. *Astronomy & Astrophysics* **584**:A48, 2015. https://doi.org/10.1051/0004-6361/201424829

[16] I. Horvath, D. Szécsi, J. Hakkila, et al. The clustering of gamma-ray bursts in the Hercules-Corona Borealis Great Wall: the largest structure in the Universe? *Monthly Notices of the Royal Astronomical Society* **498**(2):2544–2553, 2020. https://doi.org/10.1093/mnras/staa2460

[17] L. G. Balázs, Z. Bagoly, J. E. Hakkila, et al. A giant ring-like structure at $0.78 < z < 0.86$ displayed by GRBs. *Monthly Notices of the Royal Astronomical Society* **452**(3):2236–2246, 2015. https://doi.org/10.1093/mnras/stv1421

[18] L. G. Balázs, L. Rejtő, G. Tusnády. Some statistical remarks on the giant GRB ring. *Monthly Notices of the Royal Astronomical Society* **473**(3):3169–3179, 2018. https://doi.org/10.1093/mnras/stx2550

[19] Z. Bagoly, I. I. Rácz, L. G. Balázs, et al. Spatial distribution of GRBs and large scale structure of the Universe. *Proceedings of the International Astronomical Union* **11**(S319):3–4, 2015. https://doi.org/10.1017/S1743921315010820

[20] U. Andrade, C. A. P. Bengaly, J. S. Alcaniz, S. Capozziello. Revisiting the statistical isotropy of GRB sky distribution. *Monthly Notices of the Royal Astronomical Society* **490**(4):4481–4488, 2019. https://doi.org/10.1093/mnras/stz2754

[21] F. Wang, Y.-C. Zou, F. Liu, et al. A comprehensive statistical study of gamma-ray bursts. *The Astrophysical Journal* **893**(1):77, 2020. https://doi.org/10.3847/1538-4357/ab0a86

[22] S. Cao, N. Khadka, B. Ratra. Standardizing Dainotti-correlated gamma-ray bursts, and using them with standardized Amati-correlated gamma-ray bursts to constrain cosmological model parameters. *Monthly Notices of the Royal Astronomical Society* **510**(2):2928–2947, 2022. https://doi.org/10.1093/mnras/stab3559

[23] S. Cao, M. Dainotti, B. Ratra. Standardizing Platinum Dainotti-correlated gamma-ray bursts, and using them with standardized Amati-correlated gamma-ray bursts to constrain cosmological model parameters. *Monthly Notices of the Royal Astronomical Society* **512**(1):439–454, 2022. https://doi.org/10.1093/mnras/stac517

[24] J. Řípa, A. Shafieloo. Testing the isotropic universe using the gamma-ray burst data of Fermi/GBM. *The Astrophysical Journal* **851**(1):15, 2017. https://doi.org/10.3847/1538-4357/aa9708

[25] J. Řípa, A. Shafieloo. Update on testing the isotropy of the properties of gamma-ray bursts. *Monthly Notices of the Royal Astronomical Society* **486**(3):3027–3040, 2019. https://doi.org/10.1093/mnras/stz921

[26] R. Salvaterra, S. Campana, S. D. Vergani, et al. A complete sample of bright swift long gamma-ray bursts. I. Sample presentation, luminosity function and evolution. *The Astrophysical Journal* **749**(1):68, 2012. https://doi.org/10.1088/0004-637X/749/1/68

[27] A. Pescalli, G. Ghirlanda, R. Salvaterra, et al. The rate and luminosity function of long gamma ray bursts. *Astronomy & Astrophysics* **587**:A40, 2016. https://doi.org/10.1051/0004-6361/201526760

[28] J. T. Palmerio, S. D. Vergani, R. Salvaterra, et al. Are long gamma-ray bursts biased tracers of star formation? Clues from the host galaxies of the Swift/BAT6 complete sample of bright LGRBs. *Astronomy & Astrophysics* **623**:A26, 2019. https://doi.org/10.1051/0004-6361/201834179

[29] R. E. Angulo, V. Springel, S. D. M. White, et al. Scaling relations for galaxy clusters in the Millennium-XXL simulation. *Monthly Notices of the Royal Astronomical Society* **426**(3):2046–2062, 2012. https://doi.org/10.1111/j.1365-2966.2012.21830.x

[30] P. Ciarcelluti. Electrodynamic effect of anisotropic expansions in the universe. *Modern Physics Letters A* **27**(38):1250221, 2012. https://doi.org/10.1142/S0217732312502215

[31] K. Migkas, F. Pacaud, G. Schellenberger, et al. Cosmological implications of the anisotropy of ten galaxy cluster scaling relations. *Astronomy & Astrophysics* **649**:A151, 2021. https://doi.org/10.1051/0004-6361/202140296

[32] I. Horvath, I. I. Racz, Z. Bagoly, et al. Does the GRB duration depend on redshift? *Universe* **8**(4):221, 2022. https://doi.org/10.3390/universe8040221

[33] Z. Bagoly, I. Horvath, I. I. Racz, et al. The spatial distribution of gamma-ray bursts with measured redshifts from 24 years of observation. *Universe* **8**(7):342, 2022. https://doi.org/10.3390/universe8070342

[34] I. Horvath, Z. Bagoly, L. G. Balazs, et al. Mapping the Universe with gamma-ray bursts. *Monthly Notices of the Royal Astronomical Society* **527**(3):7191–7202, 2024. https://doi.org/10.1093/mnras/stad3669